International Journal on Recent and Innovation Trends in Computing and Communication
ISSN: 2321-8169 Volume: 11 Issue: 9
Article Received: *25 July 2023* ***Revised:*** *12 September 2023* ***Accepted:*** *30 September 2023*

Enhanced Antibacterial Efficacy of Chlorhexidine-Loaded Iron Oxide Nanoparticles Against *Streptococcus pneumoniae*

Rakesh Kumar[1], Renu Sharma[1], Sushila Kaura[2] Neeraj Sethi[3],

[1]Department of Chemistry, Om Sterling Global University, Hisar
[2]Department of Pharmaceutical Sciences, Atam institute of Pharmacy, OSGU, Hisar
[3]Department of Biotechnology, Om Sterling Global University, Hisar
rakesh.arora192@gmail.com
drrenu18@gmail.com
sushilakaura@gmail.com
20neerajsethi@gmail.com
*Correspondence to sushilakaura@gmail.com

Abstract

Nanoformulations offer a synergistic approach to delivering antibacterial agents. In this study, positively charged Iron nanocomplexes were developed as nanocarriers for chlorhexidine (CHX) using ionic liquids. Chlorhexidine-loaded Iron nanoparticles (CHFNPs) were thoroughly characterized using various biophysical techniques, including UV-visible spectroscopy, transmission electron microscopy, Fourier transform infrared (FTIR) spectroscopy, and zeta potential analysis. Additionally, the loading efficiency and controlled release profile of CHX from the nanocomplex were evaluated. The average diameters of Iron nanoparticles (FNPs) and CHFNPs were determined to be 27.43 nm and 29.66 nm, respectively, with CHFNPs demonstrating a sustained release of CHX, positioning them as a potent antibacterial agent. Antibacterial efficacy tests against the antibiotic-resistant Streptococcus pneumoniae strain 7465 revealed that CHFNPs significantly reduced bacterial viability. At a concentration of 100 µg/mL, CHX alone showed the highest antibacterial activity, with minimal inhibitory concentration (MIC90) and minimal bactericidal concentration (MBC96) values, followed by CHFNPs, which displayed lower MIC and MBC values. FNPs at intermediate concentrations (12 and 25 µg/mL) exhibited a bactericidal effect comparable to CHX, although they were not potent enough to completely inhibit S. pneumoniae growth. Notably, CHFNPs exhibited a significantly greater antibacterial effect than FNPs at all tested concentrations, with an MIC value of 40 µg/mL compared to 80 µg/mL for CHX. No MIC was detected for FNPs at the tested formulation concentrations. Overall, CHFNPs demonstrated a significant reduction in bacterial viability compared to CHX alone, highlighting their potential as a promising treatment option for combating infections caused by antibiotic-resistant S. pneumoniae.

Keywords: Iron nanoparticles, Chlorhexidine, Antibacterial agent, *S. pneumoniae*,

International Journal on Recent and Innovation Trends in Computing and Communication
ISSN: 2321-8169 Volume: 11 Issue: 9
***Article Received:** 25 July 2023 **Revised:** 12 September 2023 **Accepted:** 30 September 2023*

Introduction

Streptococcus pneumoniae, commonly known as pneumococcus, is a Gram-positive bacterium that plays a major role in respiratory infections, especially pneumonia. It is one of the leading causes of bacterial pneumonia, sinusitis, and otitis media, contributing significantly to the global burden of disease. A key virulence factor of this pathogen is its polysaccharide capsule, which helps it evade the host immune response. *S. pneumoniae* is transmitted through respiratory droplets and primarily colonizes the upper respiratory tract[1]. While many people carry the bacterium without symptoms, under certain conditions, it can activate its virulence, leading to infections that vary in severity from mild to potentially life-threatening. Pneumococcal diseases are particularly prevalent in young children, the elderly, and individuals with weakened immune systems.

Antibiotic resistance in *S. pneumoniae* poses a significant public health challenge, complicating the treatment of infections caused by this bacterium[1]. Over the years, the widespread use and sometimes misuse of antibiotics have exerted selective pressure on bacterial populations, fostering the emergence of resistant strains[2,3]. *S. pneumoniae*, responsible for a range of respiratory infection [4] has shown a remarkable ability to develop resistance to multiple classes of antibiotics[5] . One key factor contributing to antibiotic resistance in *S. pneumoniae* is the horizontal transfer of resistance genes, facilitated by the bacterium's capacity for genetic recombination[6]. This enables the exchange of genetic material between different strains, leading to the acquisition of resistance traits[7]. The emergence of penicillin-resistant strains was a notable early development, prompting adjustments in the treatment guidelines. The introduction of pneumococcal conjugate vaccines has played a crucial role in reducing the incidence of invasive pneumococcal diseases[8]. However, the selective pressure exerted by antibiotic use remains a concern. Resistance to macrolides, such as Erythromycin, has also been documented, which further limiting treatment options.[9] Monitoring and surveillance of antibiotic resistance pattern in *S. pneumoniae* is essential for guiding therapeutic strategies and public health interventions[10] .

The utilisation of chlorhexidine-loaded Iron oxide nanomaterials (CHFNPs) presents a promising avenue for addressing antibiotic resistance in *S. pneumoniae*. Chlorhexidine is an antiseptic with broad-spectrum activity against various microorganisms, including bacteria[11]. When incorporated into metallic nanomaterials, such as nanoparticles, it can enhance its efficacy and provide a multifaceted approach to combat antibiotic-resistant strains of *S. pneumoniae* [12]. Metallic nanomaterials, such as silver, Iron oxide, or copper nanoparticles, have inherent antimicrobial properties, making them effective agents against a range of bacteria, including antibiotic-resistant strains[13]. When combined with chlorhexidine, the synergistic effect may lead to increased antibacterial activity, potentially overcoming resistance mechanisms exhibited by *S. pneumoniae*. The nanomaterials can serve as carriers, facilitating controlled and sustained release of chlorhexidine, and optimising its therapeutic effects [14].

The nanoscale dimensions of these materials offer advantages in terms of increased surface area and enhanced penetration into the bacterial cells, allowing for more efficient interaction with the target pathogen. This targeted delivery system may minimise the potential side effects associated with systemic administration of antimicrobial agents[15]. Furthermore, the use of chlorhexidine-loaded metallic nanomaterials aligns with the principles of precision medicine, enabling tailored therapeutic approaches that specifically target the resistant strains of *S. pneumoniae*[16]. Investigations in this field are essential to optimise the formulations, dosage, and delivery mechanisms, ensuring both efficacy and safety in clinical applications. Overall, the development of such nanomaterial-based strategies represents a cutting-edge approach in the ongoing battle against antibiotic resistance in *S. pneumoniae*. Here, in this study we have designed, characterised and tested antibacterial activity of CHFNPs against antibiotic-resistant *S. pneumoniae* strain 7465. The antibacterial effects of CHFNPs

International Journal on Recent and Innovation Trends in Computing and Communication
ISSN: 2321-8169 Volume: 11 Issue: 9
***Article Received:** 25 July 2023 **Revised:** 12 September 2023 **Accepted:** 30 September 2023*

were found much better than FNPs, indicating the strong antibacterial attributes of the designed Nanoformulations.

Materials and Methods

Chemicals, compounds and Bacterium

The chlorhexidine and 1-dodecyl-3-methylimidazolium iodide were procured from MP Biomedicals, LLC, India. The compound Fe $(NO_3)_2$ was purchased from Sigma Aldrich, an establishment situated in India. Hi-media Laboratories Pvt. Ltd., Mumbai, India, supplied the culture media, penicillin, and streptomycin. Gram-positive, antibiotic-resistant bacterial strain, *Streptococcus pneumoniae* 7465 was kindly provided by the CSIR-IMTECH, Chandigarh, India. The chemicals utilised in this study were of analytical grade.

Synthesis of cationic Iron oxide nanoparticles (FNPs)

To synthesize the positively charged nanoparticles, a 1.0 mL solution of 0.1 M $Fe(NO_3)_2$ was mixed and stirred with 6.2 mM 1-dodecyl-3-methylimidazolium iodide. A 0.4 M $NaBH_4$ aqueous solution, prepared beforehand, was then added dropwise to the stirring mixture until a golden color appeared, indicating nanoparticle formation. To remove any remaining ionic liquids, the colloidal solutions were centrifuged at 8000 rpm for approximately 20 minutes[17].

Synthesis of chlorohexidine-loaded cationic Iron oxide nanoparticles (CHFNPs)

An alcoholic solution of chlorhexidine (CHX) at 1.5 mg/mL was prepared and added to an alcoholic suspension of $Fe(NO_3)_2$ at a concentration of 2 mg/mL. The mixture was stirred at room temperature for 24 hours using a magnetic stirrer. Following this, the suspension was dried in an oven at 50°C. The resulting dried product was stored in a light-protected container in a refrigerator for subsequent antibacterial investigations. Prior to conducting antimicrobial experiments, the powder was dissolved in sterile distilled water[18].

Biophysical characterisation of synthesised FNPs and CHFNPs

Various analytical tools were employed to characterise the synthesised nanoparticles. To validate the synthesis of designed nanoparticles, widely used UV-visible spectroscopy[19],[20] was employed. Distilled water was used as a benchmark control. The absorbance spectra of the colloidal sample were obtained using a UV-1800 UV-visible spectrometer manufactured by Shimadzu Corporation in Kyoto, Japan. The spectrum was measured in the wavelength range of 200 to 800 nm[21].

To ascertain the morphology, shape, and size of the designed formulations, the Transmission Electron Microscopy (TEM)[22] was used. The TEM measurements were conducted with a HITACHI H-800 microscope operating at 200 kV. To prepare the TEM grid, a small amount of the diluted solution was deposited onto a copper grid that had been covered with a layer of carbon. The solution was then dried using a lamp[23] .

The stability index of the designed formulations was monitored by Fourier Transform Infrared Spectroscopy (FT-IR spectroscopy) to categorise the substances that are responsible for both stabilising the nanoparticles and reducing the metal contents [24]. The Vertex 70 (Bruker, Germany) spectrometer, operating in the wavelength range of 400-4000 cm−1 was employed to analyse the functional group at the surface of designed formulations.

The zeta potentials of the designed nanoparticles were determined using a Zetasizer (Nano ZS-90, Malvern Instruments, UK)[25]. A total volume of 700 µL of Fe $(NO_3)_2$ suspensions was prepared and examined at 25 °C with a scattering angle of 90°.

Loading efficiency of CHX

The loading efficiency of chlorohexidine (CHX) on FNPs was assessed using UV/VIS spectroscopy[26] at a wavelength of 254 nm. The unloaded CHX amount was computed after the loading method, and the CHX loading percentage (%) was determined using the following formula:

International Journal on Recent and Innovation Trends in Computing and Communication
ISSN: 2321-8169 Volume: 11 Issue: 9
***Article Received:** 25 July 2023 **Revised:** 12 September 2023 **Accepted:** 30 September 2023*

$$\text{Loading efficiency \%} = \frac{\text{Total concentration of CHX} - \text{Concentration of unloaded CHX}}{\text{Concentration of unloaded CHX}}$$

***In vitro* release profile of CHFNPs**

To investigate the release profile of designed CHFNPs the dialysis sac method[27] was employed. A total of 10 mg of CHFNPs were placed into a dialysis sac. The sac was then submerged in a solution consisting of 10 mL of distilled water, 25% ethanol, and 0.1 M phosphate buffer saline at a pH of 7.4. The solution was continuously swirled at a rate of 100 rpm, while maintaining a constant temperature of 37 ℃. At regular intervals of 1, 2, 3, 6, 12, and 24 h, 1 mL sample was harvested and analysed using High Performance Liquid Chromatography (HPLC) with an Agilent 1200 Infinity Series instrument [28]. The analysis was performed using a ZORBAX SB C-18 column (5 µm, 150 x 4.6 mm) and a mobile phase consisting of Acetonitrile: Water (80:20 v/v). The compound of interest, Chlorohexidine, was detected at a wavelength of 254 nm, with 6.15 min retention time.

Determination of antibacterial activity of designed CHFNPs

The antibacterial attributes of the designed CHFNPs, the minimum inhibitory concentration (MIC) and the minimum bactericidal concentration (MBC) were determined against *Streptococcus pneumoniae* strain 7465 using the microdilution broth method[29], with three biological replicates. The solutions that were examined included a 0.2% concentration of CHX, a combination of FNPs and CHFNPs. The tests were performed by the guidelines set by the Clinical and Laboratory Standards Institute (CLSI). To determine the MIC, 2-fold serial dilutions (up to seven times) of the experimental solution was prepared in 96-well microtiter plates. Mueller Hinton broth (MHB) was used as negative control. To achieve a volume of 90 µL, *S. pneumoniae* was cultivated in Brain Heart Infusion (BHI) broth and the turbidity was adjusted to a range of 0.10-0.14 at an optical density (OD) of 600 nm. This resulted in a concentration of 1.6×10^6 colony forming units per millilitre (CFU/mL) of bacteria. Subsequently, the suspension was diluted at a ratio of 1 part suspension to 20 parts broth culture. A volume of 10 µL of *S. pneumoniae* suspension was introduced into each microtiter plate and plates were incubated at 37 ℃ for 24 h. Following incubation, the OD_{600} nm was recorded using a microplate reader (Biotek Micro Plate Reader).

The positive control group was comprised of culture media inoculated with *S. pneumoniae*, while the negative control group consisted of culture media devoid of *S. pneumoniae.* The MIC value was determined as the minimum concentration of each experimental solution that inhibited 90% of *S. pneumoniae* growth, in comparison to the negative control group. To measure the MBC of the designed formulations, an experimental solution with concentration equivalent to or higher than that of MIC was placed was placed on Tryptic soy Agar plates. These plates were incubated at 37 ℃ and bacterial colonies were enumerated after 24 h incubation. The MBC was determined as the lowest concentration at which the bacteria in the initial inoculum were nearly completely eradicated. This occurred when fewer than 4 discernible colonies were visible on the agar plates following 24 h incubation at 37 ℃.

Results

Bio-physical characterisation of CHFNPs nano-formulation

Particle size and Zeta potential

A comprehensive examination was performed on the FNPs and CHFNPs to ascertain their respective particle size and Zeta potential. The dimensions of the FNPs and CHFNPs were found to be 124 nm and 140.1 nm, respectively, as shown in **Fig. 1**. The Zeta potentials were measured to be +23 mV and +45.3 mV, as depicted in **Fig. 2**.

International Journal on Recent and Innovation Trends in Computing and Communication
ISSN: 2321-8169 Volume: 11 Issue: 9
Article Received: *25 July 2023* ***Revised:*** *12 September 2023* ***Accepted:*** *30 September 2023*

Percent encapsulation efficiency

The effectiveness of encapsulation depends on the molecule of interest, technique used to encapsulate materials, and media employed in the synthesis of nanoparticles[30]. The encapsulation effectiveness percentage of CHX was measured by analysing the supernatant using HPLC to quantify the quantity of unbound material. The data indicated that the encapsulation effectiveness of CHX was 70.8%. Both CHX and CHFNPs exhibit hydrophobic characteristics. They exhibit exceptional solubility in a gum solution derived from n-butanol. Consequently, the CHX was encapsulated more efficiently in nanoparticles due to this affinity.

Morphological characterisation of FNPs and CHFNPs by TEM

The FNPs and CHFNPs were isolated and exhibited a uniform spherical morphology, as evidenced by TEM **(Fig. 3)**. Their dimensions were varied between 54-68 nm for FNPs and 75 -84 nm for CHFNPs.

FTIR analysis of drug samples

The functional groups responsible for stabilising, capping, surfacing, and reducing FNPs were verified using FTIR analysis **(Fig. 4)**. The graph displays distinct peaks at 3398, 2899, and 1612 cm^{-1}, which are indicative of FNPs. The signal seen at 3398 cm^{-1} in the FNPs sample corresponds to the N-H bond of the amide and the O-H bond of the hydroxy groups, which are present on the surface imidazolium groups. In addition, the vibrations occurring at around 2899 cm^{-1} can be attributed to the stretching of aliphatic CH bonds present in the cationic aliphatic side chain. The occurrence of a peak at around 1612 cm^{-1} further substantiates the existence of an acrylic carbonyl group in FNPs. This peak also appears in the graph of CHFNPs **(Fig. 4)**.

***In vitro* drug release of CHX and CHFNPs**

Continuous nanoparticle-mediated bioactive chemical release protects against rapid metabolism and degradation[31]. The *in vitro* release profile of CHX and CHFNPs is shown in **Fig. 5**. It was found that within 4 h, 95% of pure CHX was released and because of encapsulation, CHFNPs release was more sustainable. One hour after treatment, CHFNPs release 20% CHX. Within 24 h, CHFNPs released 80% CHX. Slow release of CHX from CHFNPs, ensuring their more sustainable release.

Antimicrobial property of the CHX and CHFNPs

As per broth microdilution test, all three experimental solutions effectively suppressed the growth of *S. pneumoniae* when compared to the control group. The MIC_{90} values of all the tested solutions were comparable to their MBC_{96} values. The CHFNPs solution at a concentration of 50 µg/mL had the lowest MIC_{90} and MBC_{96} values, followed by CHX at a concentration of 100 µg/mL, and FNPs with an unspecified value. The initial concentration of FNPs was insufficient to achieve 90% inhibition of *S. pneumoniae*. Therefore, it was not possible to obtain the precise MBC_{96} and MIC_{90} values for CHFNPs. The results revealed that except for the concentration of 80 µg/mL, CHFNPs exhibited a significant decrease in bacterial viability compared to CHX. However, FNPs had a comparable antibacterial impact to CHX only at moderate concentrations (10 and 20 µg/mL), and their effects were significantly inferior to those of CHX at all other concentrations (3, 6, 40, and 80 µg/mL). The effects of CHFNPs were significantly superior to those of FNPs at all tested concentrations **(Fig. 6 and Table 1)**.

Discussion

Nanoparticles have wide applications in medical field, but more recent interest has arisen primarily in the response to emerging field of drug delivery systems, where it is being used as nanocarriers. At present many drugs fail in clinical trials because the compound cannot be delivered to the site where it is needed without having some interaction with the human body. The result can range from triggering a severe immune response to toxic side effects. Getting the active drug/compound to where it is required, and effectively delivering it are one of the holy grails in the treatment of diseases, ranging from inflammations to bacterial infections.

International Journal on Recent and Innovation Trends in Computing and Communication
ISSN: 2321-8169 Volume: 11 Issue: 9
***Article Received:** 25 July 2023 **Revised:** 12 September 2023 **Accepted:** 30 September 2023*

The global pharmaceutical industry has been developing compounds for over a century, but many of these are not so effective. Considering this objective in mind, we have developed Chlorohexidine-loaded Iron oxide nanoparticles (CHFNPs) and monitored their antibacterial attributes on Gram-positive, antibiotic-resistant bacterial strain, *S. pneumoniae* 7465.

Customising the size, shape, and/or surface chemistry of nanoparticles enables them to fulfil various needs[32]. The intended action of nanoparticles depends on their target organ or tissue. Both tumour permeability and efficient cellular absorption of nanoparticles, which are dependent on their size, are prerequisites for nanotherapeutics [33] . Furthermore, influencing the ideal size of a nanoparticle is the target site and the kind of targeted tissue [34]. Many size-dependent phenomena including chemical, electrical, magnetic, and mechanical characteristics are introduced by the high surface-to-volume ratio of nanoparticles combined with size effects (quantum effects). Since particle size is so important to nanoparticle properties, particle size is a necessary step in characterising nanoparticle qualities[35]. The obtained particle size of CHFNPs ranging from 124 to 140.1 nm in our study suggests a stable nano-formulation.

The zeta potential (ζ) is a surface charge measurement and the scientific term for electrokinetic potential in colloidal systems [36]. Particle stability as well as cellular absorption and intracellular trafficking can be affected. An electrical double layer and van der Waals forces working in balance determine the stability of a colloidal system where Zeta potential of nanocarriers is crucial. It provides data on particle charge and particle tendency in a formulation to aggregate or stay discrete and is obtained using a Zetasizer or other methods[37]. In general, particles that have Zeta potential greater than +30 mV or greater than −30 mV are regarded to be stable[38]. The attracting forces cause the emulsion droplets or colloids to gather if the Zeta potential drops below a specific threshold. On the other hand, a stable system is maintained by a high Zeta potential (either positive or negative), usually more than 30 mV[39]. While repulsion between particles with identical electric charges prevents particle aggregation and assurances easy redispersion, extremely positive or negative Zeta potential values produce stronger repulsive forces[40]. In our study, Zeta potential of Chlorohexidine (CHX) and CHFNPs was measured to be +23 mV and +45.3 mV, respectively, demonstrating the generated nano-formulations were rather stable. We found that CHX was encapsulated in the CHFNPs quite effectively with a 70.8% efficacy. The encapsulation efficiency percentage of a nanoparticle indicates how much of a nano-formulation is effectively encapsulated[41]. Its computation is the total drug added less the free, non-entrapped drug multiplied by 100. Moreover, important is the drug release time course from nanoparticles, which establishes the quantity of free drug available over time[42]. The toxicity profile of the formulation may either be altered, or it could have a therapeutic benefit by free drug. Previous studies indicated that the percentage of energy efficiency increased from 78.63 ± 4.2% to 87.93 ± 11.4% in direct proportion to the increase in CHX accumulation during PLGA/CHX formulation preparation and an encapsulation efficiency of 78.63 ± 4.2% led to a drug-loading of 10.49 ± 1.37%, which dramatically increased to a high of 19.26 ± 7.42% when more CHX was added, resulting in a ratio of 125:50[43].

TEM analysis provides valuable insights into various aspects of the sample, including sample size, particle size statistics, crystal grain size, crystal structure, crystal phase composition, and atomic arrangement order[44]. The size of nanoparticles influences their release rate. TEM measures the size of the particles in a dehydrated and isolated atmosphere, resulting in a decrease in particle size[45]. The TEM analysis determined the respective size of FNPs and CHFNPs ranged from 54-68 nm and 75-84 nm, indicating stable nano-formulations. Nanoparticles are distributed throughout various organs in the body based on their specific structure and size. The form and size of nanoparticles have a crucial role in determining their longevity, compatibility with living organisms, and capacity to penetrate biological tissue. Nanoparticles of smaller sizes exhibit increased durability in

International Journal on Recent and Innovation Trends in Computing and Communication
ISSN: 2321-8169 Volume: 11 Issue: 9
***Article Received:** 25 July 2023 **Revised:** 12 September 2023 **Accepted:** 30 September 2023*

the bloodstream compared to nanoparticles of larger sizes. In a previous study, TEM analysis indicated that the average size of AgNPs+ and CHX@AgNPs+ nanoformulations was roughly the same[46]. Respective mean diameters of AgNPs+ and CHX@AgNPs+ was determined to be of 27.43 nm and 29.66 nm.

The FTIR analysis of the CHFNPs suggests the designed nanoformulations was stable. FTIR spectroscopy is a versatile technique, measure a wide range of frequencies[47]. The use of this technique encompasses several methods for examining nanomaterials, such as discerning their specific type and composition, ascertaining their level of purity and quality, tracking the progress of their synthesis and processing, evaluating the features of their surface and interface, and investigating the interactions and impacts of these nanoparticles[48]. FTIR spectroscopy quantifies molecular vibrations and rotations induced by infrared radiation of a particular wavelength. It can detect alterations in functional groups inside biomolecules and ascertain the chemical makeup of the surface of a nanoparticle. FTIR spectroscopy can be employed to observe and analyse chemical processes occurring on the surface of nanoparticles, considering different factors including temperature and the surrounding gaseous conditions[49]. In previous studies, Free/MNP@CHX immobilised FTIR, the Aminosilane shell surrounding the magnetic core displayed a large band at 3,355 and 3,393 cm−1 in both samples, indicating N-H stretching and bending vibrations. Moderate signals are produced by NH wagging at 868 cm−1 for CHX and 847 cm−1 for MNP@CHX. In biguanide derivatives, C=N stretching vibrations may produce adsorption bonds at 1,600 cm−1 [50]. In our study, FNP peaks appear at 3398, 2899, and 1612 cm^{-1}. The imidazolium groups' surface amide and hydroxy groups' N-H and O-H bonds are visible at 3398 cm-1 in the FNPs sample. The cationic aliphatic side chain's aliphatic CH bands stretch, causing vibrations at 2899 cm^{-1}. A peak at 1612 cm^{-1} supports FNPs' acrylic carbonyl group.

Evaluation of *in vitro* drug release is an essential parameter to evaluate the quality, safety, and effectiveness of any drug delivery systems that utilise nanoparticles[51]. Many instruments are utilised to quantify the accessibility of drugs during the initial phases of product development, ensuring quality control for batch release, evaluate factors related to formulation, assess manufacturing methods that impact bioavailability[52], which determine the pharmaceutical quality of a product, and monitor formulation design and batch-to-batch variation. Here we found that within 24 h, CHFNPs released 80% CHX indicating a sustainable release of nanoparticles.

Nanoparticles exhibit antibacterial and biocidal characteristics, allowing them to effectively battle bacteria, fungi, and viruses[53]. Here we found that the antibacterial effect of the designed nano-formulation, CHFNPs on *S. pneumoniae* 7465 was much higher than that of FNPs alone at all tested concentrations, indicating CHFNPs hold strong antibacterial property.

The constant release of CHX from CHFNPs, made our nano-formulations more effective antibacterial agent at least for the *S. pneumoniae* 7465. Nanoparticles exhibit properties that make them very appropriate as antimicrobial agents, including a large surface area, charge, ability to deliver a big amount of antibiotics or other compounds, size, and shape[54]. Previous study demonstrated that CHX@AgNPs+ nanoformulations had a much greater antibacterial impact, reducing the bacterial viability as compared to CHX [55]. The AgNPs+ exhibited comparable antibacterial properties to CHX only at moderate doses (12-25 µg/mL), whereas their effectiveness was much lower than that of CHX at other concentrations (3, 6, 50, and 100 µg/mL). The MIC values of CHX@AgNPs+ and CHX were found to be 50 and 100 µg/mL, respectively[56].

Considerable efforts have been made to assess the antiseptic efficacy of new nano-formulations carrying CHX as main antimicrobial agent. Based on the current situation and the results obtained from our *in vitro* study, we accentuate the need for additional research on the use of these CHX loaded nano-formulations. In summary, here we created a CHX carrying CHFNPs nano-formulation that has substantial

International Journal on Recent and Innovation Trends in Computing and Communication
ISSN: 2321-8169 Volume: 11 Issue: 9
Article Received: *25 July 2023* ***Revised:*** *12 September 2023* ***Accepted:*** *30 September 2023*

antibacterial effect against the Gram-positive, antibiotic-resistant bacterium, *S. pneumoniae* 7465.

Conclusion

The CHX nano-formulation demonstrated superior efficacy *in vitro*, requiring lower amounts of CHX compared to commercially available CHX products. Our study demonstrates that CHX carrying CHFNPs nanoformulation possesses suitable physicochemical characteristics, as well as antibacterial properties. Collectively, our findings indicate that CHFNPs show promise as a potential alternative nanoformulation. Our results have shown significant positivity, which supports the advancement of future pharmacological investigations to determine the mechanisms of action of the nanostructured formulation. Additionally, these results are encouraging for evaluating various concentrations of CHX in different nanoformulations, as well as assessing the penetration mechanisms and potential toxicity of these nano-formulations.

Author Contribution: R.S, and S.K. proposed the concept of manuscript; R.K. investigated the study, collected data, and prepared the initial draft of the manuscript; I.S. contributed to manuscript writing and analysis of data; D.K.G. and N.S. directed the manuscript writing and refined the drafts of the manuscript. All authors have read and agreed to the published version of the manuscript.

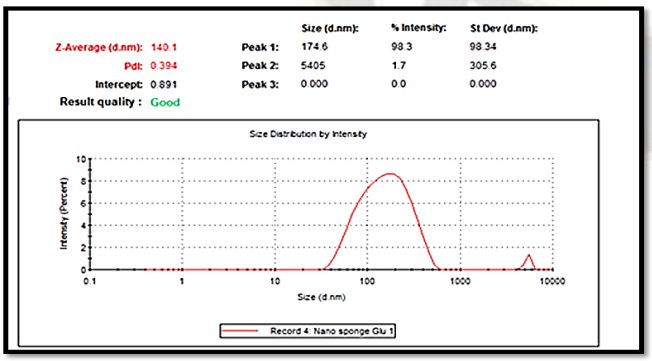

Figure 1: Particle size analysis of CHX carrying CHFNPs nanoformulation. The Mastersizer 3000+ serves as a dependable companion for conducting particle size analysis. The CHFNPs wasfound to be \ 140.1 nm

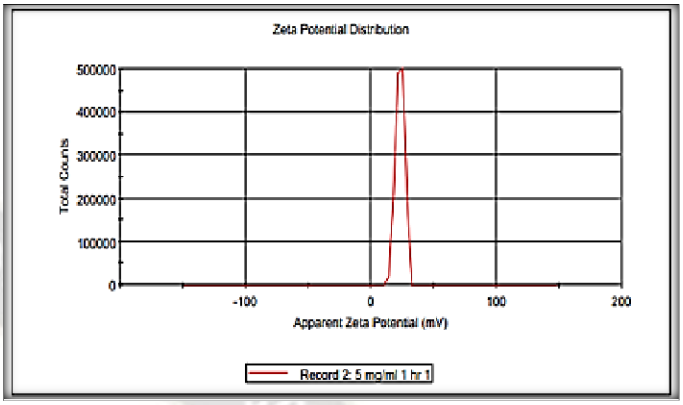

Figure 2: Zeta Potential of CHX carrying CHFNPs nanoformulation. The zeta potentials of the designed nanoparticles were determined using a Zetasizer (Nano ZS-90, Malvern Instruments, UK. The Zeta potentials were measured to be +23 mV and +45.3 mV.

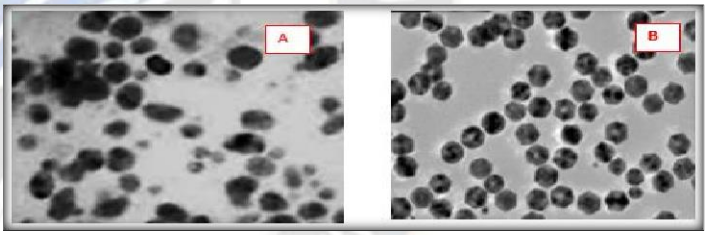

Figure 3: TEM analysis of Fe nanoparticles (A) and CHX carrying CHFNPs nanoformulation (B). The TEM measurements were conducted with a HITACHI H-800 microscope operating at 200 kV. To prepare the TEM grid, a small amount of the diluted solution was deposited onto a copper grid that had been covered with a layer of carbon. The solution was then dried using a lamp. Their Dimensions of FNPs and CHFNPs were varied between 54-68 nm for FNPs and 75 -84 nm for CHFNPs.

International Journal on Recent and Innovation Trends in Computing and Communication
ISSN: 2321-8169 Volume: 11 Issue: 9
Article Received: *25 July 2023* ***Revised:*** *12 September 2023* ***Accepted:*** *30 September 2023*

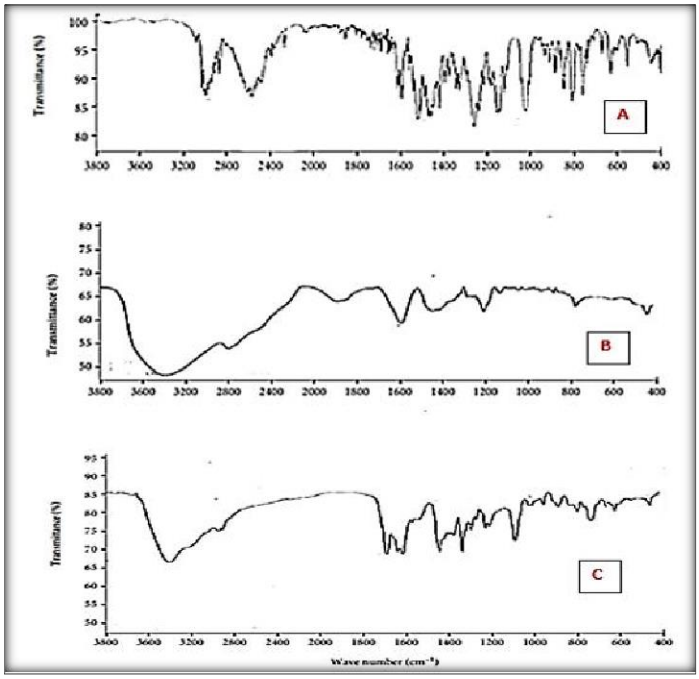

Figure 4: FT-IR spectra of Chlorhexidine, CHX (A), Fe nanoparticles (B), and CHX-carrying CHFNPs nanoformulation (C). The Vertex 70 (Bruker, Germany) spectrometer, operating in the wavelength range of 400-4000 cm−1 was employed to analyse the functional group at the surface of designed formulations. FNP peaks appear at 3398, 2899, and 1612 cm-1 in the graph. The imidazolium groups' surface amide and hydroxy groups' N-H and O-H bonds are visible at 3398 cm-1 in the FNPs sample. The cationic aliphatic side chain's stretching of aliphatic CH bonds causes vibrations at 2899 cm-1. A peak at 1612 cm-1 supports FNPs' acrylic carbonyl group. CHFNP graphs show this peak.

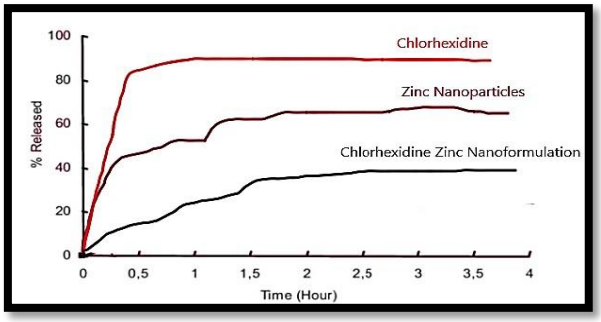

Figure 5: *In vitro* release profile of Chlorhexidine, Fe nanoparticles and CHX carrying CHFNPs

nanoformulation Dialysis sacs were used to examine anticipated CHFNP release. A dialysis bag had 10 mg CHFNPs. The sac was then submerged in 10 mL distilled water, 25% ethanol, and 0.1 M pH 7.4 phosphate buffer saline. The solution stayed at 37 °C by swirling at 100 rpm. HPLC using an Agilent 1200 Infinity Series analysed 1 mL samples at 1, 2, 3, 6, 12, and 24 h. Analyses were performed on a 5 µm ZORBAX SB C-18 column (150 x 4.6 mm) using an 80:20 v/v Acetonitrile: Water mobile phase. With 6.15 min retention, chlorohexidine was detected at 254 nm. In vitro CHX and CHFNP release profiles are depicted in Fig. 5. Encapsulation made CHFNPs release more sustainably and 95% of pure CHX was released in 4 h. One hour post-treatment, CHFNPs release 20% CHX. In 24 hours, CHFNPs released 80% CHX. Slow CHX emission from CHFNPs ensures sustainability.

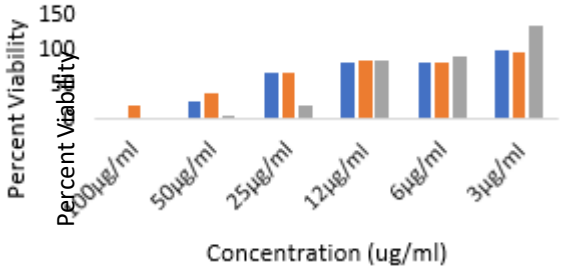

Figure 6: Viability of *Streptococcus pneumoniae* when treated with different concentrations of designed nanoformulations Three biological replicates were used to determine the minimum inhibitory concentration (MIC) and minimum bactericidal concentration (MBC) of the proposed CHFNPs against Streptococcus pneumoniae strain 7465 using the microdilution broth method. The tested solutions contained 0.2% CHX, FNPs, and CHFNPs. Clinical and Laboratory Standards Institute guidelines guided the tests. In the broth microdilution test, all three experimental solutions reduced S. pneumoniae growth better than the control group. All tested solutions

exhibited identical MIC90 and MBC96. CHFNPs solution at 50 µg/mL had the lowest MIC90 and MBC96 values, followed by CHX at 100 µg/mL and FNPs with an unknown value. Initial FNP concentration did not block S. pneumoniae 90%. The CHFNP MBC96 and MIC90 values were unknown. Research indicates that CHFNPs dramatically lower bacterial viability compared to CHX, except at 80 µg/mL concentration. The bactericidal effects of FNPs were comparable to CHX at intermediate levels (10 and 20 µg/mL), but much less at higher concentrations (3, 6, 40, and 80 µg/mL). At all concentrations, CHFNPs outperformed FNPs.

Table 1: Viability of *S. pneumoniae* following treatment with different concentrations of designed nanoformulations.

	Percent (%) viability at various concentration (µg/mL)					
Nanoformulation	**100 µg/mL**	**50 µg/mL**	**25 µg/mL**	**12 µg/mL**	**6 µg/mL**	**3 µg/mL**
CHX	4	24	64	80	80	96
FNPs	18	38	64	82	80	94
CHX + FNPs	2	6	18	82	86	130

References

[1] Sethi, N., Bhardwaj, P., Kumar, S., Dilbaghi, N. (2019). Development And Evaluation Of Ursolic Acid Loaded Eudragit-E Nanocarrier For Cancer Therapy. *International Journal of Pharmaceutical Research (09752366), 11*(2

[2] ElMansy, M. M., Tadros, S. S. T., Saleh, R. S., Abdelmonem, R., El Menoufy, H., Shawky, N. (2023). Comparative evaluation on the effect of different cavity disinfectant nano gels; Chlorohexidine, Propolis, Liquorice versus Diode Laser in terms of composite microleakage (comparative in vitro study). *BDJ open*, *9*(1), 49

[3] Saini, A., Budania, L. S., Berwal, A., Sethi, S. K. N. (2023). Screening of the Anticancer Potential of Lycopene-Loaded Nanoliposomes. *Tuijin Jishu/Journal of Propulsion Technology*, *44*(4), 1372-1383

[4] Nasef, A., Jamil, W., Mosleh, A. A., Elshatory, E. H. (2023). Comparative Study of the Synergistic Antimicrobial Efficacy of Chitosan with Chlorhexidine, Silver, and Propolis in Human Saliva. *Al-Azhar Dental Journal for Girls*, *10*(1), 83-91

[5] Dhanda, P., Sura, S., Lathar, S., Shoekand, N., Partishtha, H., Sethi, N. (2022). Traditional, phytochemical, and biological aspects of Indian spider plant

[6] Delfani, S., Shakibaie, M., Lornejad, A., Zadeh, R. Y. (2022). Potent effects of green synthesized Iron oxide nanoparticles against some cariogenic bacteria (Streptococcus mutans and Actinomyces viscosus). *Global Journal of Medical, Pharmaceutical, and Biomedical Update*, *17*

[7] Wassel, M., Radwan, M., Elghazawy, R. (2023). Direct and residual antimicrobial effect of 2% chlorhexidine gel, double antibiotic paste and chitosan-chlorhexidine nanoparticles as intracanal medicaments against Enterococcus faecalis and Candida albicans in primary molars: an in-vitro study. *BMC Oral Health*, *23*(1), 296

[8] Scelfo, C., Menzella, F., Fontana, M., Ghidoni, G., Galeone, C., & Facciolongo, N. C. (2021). Pneumonia and invasive pneumococcal diseases: the role of pneumococcal conjugate vaccine in the era of multi-drug resistance. Vaccines, 9(5), 420.

9 Alvarez-Elcoro, S., & Enzler, M. J. (1999, June). The macrolides: erythromycin, clarithromycin, and azithromycin. In Mayo Clinic Proceedings (Vol. 74, No. 6, pp. 613-634). Elsevier.

[10] Kaura, S., Parle, M., Insa, R., Yadav, B. S., Sethi, N. (2022). Neuroprotective effect of goat milk. *Small Ruminant Research*, *214*, 106748

[11] Noor, S. S. S. E. (2016). Chlorhexidine: Its properties and effects. *Research Journal of Pharmacy and Technology*, *9*(10), 1755-1760.

[12] Steckiewicz, K. P., Cieciórski, P., Barcińska, E., Jaśkiewicz, M., Narajczyk, M., Bauer, M., Inkielewicz-Stepniak, I. (2022). Silver nanoparticles as chlorhexidine and metronidazole drug delivery platforms: their potential use in treating periodontitis. *International journal of nanomedicine*, 495-517

[13] Sánchez-López, E., Gomes, D., Esteruelas, G., Bonilla, L., Lopez-Machado, A. L., Galindo, R., ... & Souto, E. B. (2020). Metal-based nanoparticles as antimicrobial agents: an overview. *Nanomaterials*, *10*(2), 292.

[14] Kumar, R., Sethi, N., Kaura, S. (2022). Bio-processing and analysis of mixed fruit wine manufactured using Aegle marmelos and Phoenix dactylifer

[15] Leeyaphan, C., Kulthanachairojana, N., Taychakhoonavudh, S., Chanyachailert, P., Kobkurkul, P., Buranaporn, P., Bunyaratavej, S. (2023). Randomized controlled trial and cost-effectiveness analysis: Comparing chlorhexidine scrub, FeO-nanoparticle socks, and their combination in pitted keratolysis treatment. *The Journal of Dermatology*, *50*(11), 1427-1432

[16] Poonam, D., Sethi, N., Pal, M., Kaura, S., Parle, M. (2014). Optimization of shoot multiplication media for micro propagation of Withania somnifera: an endangered medicinal plant. *Journal of Pharmaceutical and Scientific Innovation (JPSI)*, *3*(4), 340-343

[17] Shirazi, M., Qazvini, F. F., Mohamadrezaie, S. (2023). Antimicrobial properties of glass-ionomer cement incorporated with zinc oxide nanoparticles against mutans streptococci and lactobacilli under orthodontic bands: An in vivo split-mouth study. *Dental Research Journal*, *20*

[18] Suman, J., Neeraj, S., Rahul, J., Sushila, K. (2014). Microbial synthesis of silver nanoparticles by Actinotalea sp. MTCC 10637. *American Journal of Phytomedicine and Clinical Therapeutics*, *2*, 1016-23

[19] Patil, R. B., & Chougale, A. D. (2021). Analytical methods for the identification and characterization of silver nanoparticles: A brief review. *Materials Today: Proceedings*, *47*, 5520-5532.

[20] Patil, R. B., & Chougale, A. D. (2021). Analytical methods for the identification and characterization of silver nanoparticles: A brief review. *Materials Today: Proceedings*, *47*, 5520-5532.

[21] Delfani, S., Shakibaie, M., Lornejad, A., Zadeh, R. Y. (2022). Potent effects of green synthesized zinc nanoparticles against some cariogenic bacteria (Streptococcus mutans and Actinomyces viscosus). *Global Journal of Medical, Pharmaceutical, and Biomedical Update*, *17*

[22] Milind, P., Sushila, K., Neeraj, S. (2013). Understanding gout beyond doubt. *International Research Journal of Pharmacy*, *4*(9), 25-34

[23] Sethi, N., Kaura, S., Dilbaghi, N., Parle, M., Pal, M. (2014). Garlic: A pungent wonder from nature. *International research journal of pharmacy*, *5*(7), 523-529

[24] Moshrefi, A. (2002, January). Chlorhexidine. In *The Journal of the Western Society of Periodontology/periodontal Abstracts* (Vol. 50, No. 1, pp. 5-9)

[25] Marsalek, R. (2014). Particle size and zeta potential of FeO. *APCBEE procedia*, *9*, 13-17.

[26] Milind, P., Renu, K., Kaura, S. (2013). Non-behavioral models of psychosis. *International Research Journal of Pharmacy*, *4*(8), 89-95

[27] Bhardwaj U, Burgess DJ. Physicochemical properties of extruded and non-extruded liposomes containing the hydrophobic drug dexamethasone. *Int J Pharm.* 2010;388(1–2):181–9

[28] Oliveira, H. M., De Sousa Silva, F. A., Lins Almeida Barbosa, T., Freire Rodrigues, M. G. (2023). Sustainable Synthesis of Zeolitic Imidazolate Framework-8 Nanoparticles and Application in the Adsorption of the Drug Chlorhexidine. *Catalysis Research*, *3*(1), 1-15

[29] Eriksen, H. B., Fuursted, K., Jensen, A., Jensen, C. S., Nielsen, X., Christensen, J. J., ... & One Day in Denmark (ODiD) Consortium. (2023). Predicting β-lactam susceptibility from the genome of Streptococcus pneumoniae and other mitis group streptococci. *Frontiers in Microbiology*, *14*, 1120023.

[30] Alaghehmad, H., Mansouri, E., Esmaili, B., Bijani, A., Nejadkarimi, S., Rahchamani, M. (2018). Effect of 0.12% chlorhexidine and zinc nanoparticles on the microshear bond strength of dentin with a fifth-generation adhesive. *European Journal of Dentistry*, *12*(01), 105-110

[31] Yang, C., & Merlin, D. (2019). Nanoparticle-mediated drug delivery systems for the treatment of IBD: current perspectives. *International journal of nanomedicine*, 8875-8889.

[32] Albanese, A., Tang, P. S., & Chan, W. C. (2012). The effect of nanoparticle size, shape, and surface chemistry on biological systems. *Annual review of biomedical engineering*, *14*, 1-16.

[33] Swain, S., Kumar Sahu, P., Beg, S., & Manohar Babu, S. (2016). Nanoparticles for cancer targeting: current and future directions. *Current drug delivery*, *13*(8), 1290-1302.

[34] De Crozals, G., Bonnet, R., Farre, C., & Chaix, C. (2016). Nanoparticles with multiple properties for biomedical applications: A strategic guide. *Nano Today*, *11*(4), 435-463.

[35] Lu, Z., & Yin, Y. (2012). Colloidal nanoparticle clusters: functional materials by design. *Chemical Society Reviews*, *41*(21), 6874-6887.

[36] Clogston, J. D., & Patri, A. K. (2011). Zeta potential measurement. *Characterization of nanoparticles intended for drug delivery*, 63-70.

[37] Kaszuba, M., Corbett, J., Watson, F. M., & Jones, A. (2010). High-concentration zeta potential measurements using light-scattering techniques. *Philosophical transactions of the royal society a: mathematical, physical and engineering sciences*, *368*(1927), 4439-4451.

[38] Berg, J. M., Romoser, A., Banerjee, N., Zebda, R., & Sayes, C. M. (2009). The relationship between pH and zeta potential of~ 30 nm metal oxide nanoparticle suspensions relevant to in vitro toxicological evaluations. *Nanotoxicology*, *3*(4), 276-283.

[39] Smith, M. C., Crist, R. M., Clogston, J. D., & McNeil, S. E. (2017). Zeta potential: a case study of cationic, anionic, and neutral liposomes. *Analytical and bioanalytical chemistry*, *409*, 5779-5787.

[40] Anderson, W., Kozak, D., Coleman, V. A., Jämting, Å. K., & Trau, M. (2013). A comparative study of submicron particle sizing platforms: accuracy, precision and resolution analysis of polydisperse particle size distributions. *Journal of colloid and interface science*, *405*, 322-330.

[41] Song, X., Zhao, Y., Hou, S., Xu, F., Zhao, R., He, J., ... & Chen, Q. (2008). Dual agents loaded PLGA nanoparticles: systematic study of particle size and drug entrapment efficiency. *European journal of pharmaceutics and biopharmaceutics*, *69*(2), 445-453.

[42] Zhang, Z., & Feng, S. S. (2006). The drug encapsulation efficiency, in vitro drug release, cellular uptake and cytotoxicity of paclitaxel-loaded poly (lactide)–tocopheryl polyethylene glycol succinate nanoparticles. *Biomaterials*, *27*(21), 4025-4033.

[43] Priyadarshini, B. M., Mitali, K., Lu, T. B., Handral, H. K., Dubey, N., & Fawzy, A. S. (2017). PLGA nanoparticles as chlorhexidine-delivery carrier to resin-dentin adhesive interface. *Dental Materials*, *33*(7), 830-846.

[44] Beganskienė, A., Sirutkaitis, V., Kurtinaitienė, M., Juškėnas, R., & Kareiva, A. (2004). FTIR, TEM and NMR investigations of Stöber silica nanoparticles. *Mater Sci (Medžiagotyra)*, *10*(4), 287-290.

[45] Rauwel, P., Küünal, S., Ferdov, S., & Rauwel, E. (2015). A review on the green synthesis of silver nanoparticles and their morphologies studied via TEM. *Advances in Materials Science and Engineering*, *2015*.

[46] Tülü, G., Kaya, B. Ü., Çetin, E. S., & Köle, M. (2021). Antibacterial effect of silver nanoparticles mixed with calcium hydroxide or chlorhexidine on multispecies biofilms. *Odontology*, *109*(4), 802-811.

[47] Dutta, A. (2017). Fourier transform infrared spectroscopy. *Spectroscopic methods for nanomaterials characterization*, 73-93.

[48] Bates, J. B. (1976). Fourier Transform Infrared Spectroscopy: The basic principles and current applications of a rapidly expanding technique are reviewed. *Science*, *191*(4222), 31-37.

[49] Hsu, C. P. S. (1997). Infrared spectroscopy. *Handbook of instrumental techniques for analytical chemistry*, *249*.

[50] Tokajuk, G., Niemirowicz, K., Deptuła, P., Piktel, E., Cieśluk, M., Wilczewska, A. Z., ... & Bucki, R. (2017). Use of magnetic nanoparticles as a drug delivery system to improve chlorhexidine antimicrobial activity. *International journal of nanomedicine*, 7833-7846.

[51] Weng, J., Tong, H. H., & Chow, S. F. (2020). In vitro release study of the polymeric drug nanoparticles: development and validation of a novel method. *Pharmaceutics*, *12*(8), 732.

[52] Ragelle, H., Danhier, F., Préat, V., Langer, R., & Anderson, D. G. (2017). Nanoparticle-based drug delivery systems: a commercial and regulatory outlook as the field matures. *Expert opinion on drug delivery*, *14*(7), 851-864.

[53] Sharmin, S., Rahaman, M. M., Sarkar, C., Atolani, O., Islam, M. T., & Adeyemi, O. S. (2021). Nanoparticles as antimicrobial and antiviral agents: A literature-based perspective study. *Heliyon*, *7*(3).

[54] Salleh, A., Naomi, R., Utami, N. D., Mohammad, A. W., Mahmoudi, E., Mustafa, N., & Fauzi, M. B. (2020). The potential of silver nanoparticles for antiviral and antibacterial applications: A mechanism of action. *Nanomaterials*, *10*(8), 1566.

[55] Charannya, S., Duraivel, D., Padminee, K., Poorni, S., Nishanthine, C., & Srinivasan, M. R. (2018). Comparative Evaluation of Antimicrobial Efficacy of Silver Nanoparticles and 2% Chlorhexidine Gluconate When Used Alone and in Combination Assessed Using Agar Diffusion Method: An: In vitro: Study. *Contemporary clinical dentistry*, *9*(Suppl 2), S204-S209.

[56] Gompers, E. (2023). *A Comparison of the Effects of Chlorhexidine Hexametaphosphate and Silver Nanoparticle Antimicrobials on the Mechanical and Esthetic Properties of Elastomeric Chain* (Doctoral dissertation, State University of New York at Buffalo).